JOURNAL OF GUIDANCE, CONTROL, AND DYNAMICS
Vol. 33, No. 6, November–December 2010

Cooperative Multiple-Model Adaptive Guidance for an Aircraft Defending Missile

Vitaly Shaferman* and Tal Shima†
Technion—Israel Institute of Technology, Haifa 32000, Israel

DOI: 10.2514/1.49515

A cooperative guidance law is presented for a defender missile protecting an aerial target from an incoming homing missile. The filter used is a nonlinear adaptation of a multiple-model adaptive estimator, in which each model represents a possible guidance law and guidance parameters of the incoming homing missile. Fusion of measurements from both the defender missile and protected aircraft is performed. A matched defender's missile guidance law is optimized to the identified homing-missile guidance law. It uses cooperation between the aerial target and the defender missile. The cooperation stems from the fact that the defender knows the future evasive maneuvers to be performed by the protected target and thus can anticipate the maneuvers it will induce on the incoming homing missile. Moreover, the target performs a maneuver that minimizes the control effort requirements from the defender. The estimator and guidance law are combined in a multiple-model adaptive control configuration. Simulation results show that combining the estimations with the proposed optimal guidance law, which uses cooperation between the defending missile and protected target, yields hit-to-kill closed-loop performance with very low control effort. This facilitates the use of relatively small defending missiles to protect aircraft from homing missiles.

Nomenclature

$\mathbf{A}$, $\mathbf{B}$, $\mathbf{C}$ = linearized guidance-problem state-space model matrices
$\mathbf{A}_d$, $\mathbf{B}_d$, $\mathbf{C}_d$, D_d = defender's dynamics state-space model matrices during the endgame
a = normal acceleration
b = weight
$\mathbf{D}$ = constant vector
$\mathbf{F}_x$ = dynamics Jacobian matrix
$\mathbf{f}_{k-1}$ = discrete-time equations of motion
f_s = measurement sampling rate
H = Hamiltonian
$\mathbf{H}_x$ = measurement Jacobian matrix
$\mathbf{h}_k$ = measurement function
J = cost function
J_c = cost function for cooperative optimal guidance law
$\mathbf{K}_k$ = Kalman gain
$\mathcal{N}$ = Gaussian distribution
N' = navigation gain
$\mathbf{P}$ = covariance
$\mathbf{Q}_d$ = covariance matrix of the equivalent discrete process noise
$\mathbf{R}$ = measurement covariance matrix
r = missile regime
$\mathbf{S}$ = innovation covariance matrix
s = number of possible regimes/filters
t = time
t_f = final time
t_{go} = time-to-go
t_{sw} = target switch time
u = acceleration command
V = speed
V_λ = speed perpendicular to line of sight
V_ρ = speed along line of sight
$\boldsymbol{v}_k$ = measurement noise at time t_k
$\boldsymbol{x}$ = state vector
$\hat{\boldsymbol{x}}$ = state estimate
x, y = position states
$\boldsymbol{x}_k$ = relative defender–missile state vector at time t_k
$\boldsymbol{y}$ = state vector of the linearized guidance problem
$\boldsymbol{y}_d$ = defender's internal state vector
Z = zero-effort miss
$\boldsymbol{z}_k$ = measurement vector at time t_k
$\mathcal{Z}_k$ = measurement history up to time k
α, β = ratio between the weight on the control effort and the miss distance
θ, η = normalized time-to-go
γ = flight-path angle
Λ_k^j = jth-regime-conditioned likelihood function at t_k
λ = line-of-sight angle
λ_z = zero-effort-miss costate
μ_k^j = posterior probability at t_k that the jth regime is correct
ν = innovation
ξ = relative displacement between the defender and the missile
ρ = range
σ^2 = measurement noise variance
τ = time constant
$\mathbf{\Phi}$ = transition matrix
ψ = time-varying function

Subscripts

APN = augmented proportional navigation
COGL = cooperative optimal guidance law
d = defender
dm = relative defender–missile states
k = discrete time t_k
m = missile
OGL = optimal guidance law
OSCOGL = optimal-switch cooperative optimal guidance law
PN = proportional navigation

Received 21 February 2010; revision received 7 May 2010; accepted for publication 7 May 2010.

*Doctoral Student, Department of Aerospace Engineering; vitalysh@tx.technion.ac.il.

†Senior Lecturer, Department of Aerospace Engineering; tal.shima@technion.ac.il. Associate Fellow AIAA.

t	=	target
tm	=	relative target–missile states
0	=	initial conditions

Superscripts

c	=	command
I	=	inertial coordinate frame
j, i	=	jth, ith filter/regime
n	=	normal to LOS_0
R	=	relative coordinate frame

I. Introduction

IN THE last half-century there has been substantial advancement in the field of missile guidance. From the well-known proportional navigation (PN) guidance law [1] to the augmented PN (APN) guidance law [2], optimal guidance law (OGL) [3] and differential-game-based guidance laws, such as the linear quadratic differential-game guidance law [4,5], and bounded control differential-game guidance laws (DGL/0, DGL/1) [6,7].

To counter this advancement, in interceptor missile guidance, there has been a considerable effort to develop target-evasion guidance laws, in an attempt to increase aircraft survivability. These target-evasion guidance laws can be roughly divided into two categories: those that assume that the target has perfect information on the interceptor's initial conditions and state vector [6–17] and those that do not rely on this assumption [18–22].

The first category of target-evasion guidance laws, which assume perfect information, were traditionally formulated in two forms, either as a differential game [8,9] or as a one-sided optimization optimal control problem. In the former the problem is formulated as a perfect-information zero-sum pursuit–evasion game [6,7]. The solution of the game yields the perfect-information strategy for both the pursuer and the evader and the value of the game (the miss distance guaranteed to the pursuer, as well as to the evader, by using the respective optimal strategies). This formulation assumes worst case for both the pursuer and the evader and is therefore conservative if the evader has some a priori information about the pursuer's strategy.

Knowledge of the pursuer's strategy gives the evader an advantage. As PN is the most widely operationally used guidance law, most perfect-information evasion laws were formulated as a one-sided optimal control problem against a PN-guided interceptor. This problem is nonlinear and three-dimensional, and both the pursuer and the evader have nonideal dynamics with acceleration limits. An analytical solution of the full problem is unrealistic. Therefore, the solutions proposed were obtained by applying different simplifying assumptions and using numerical solution schemes. The typical simplifying assumptions in these studies included linearization around the collision course [11–13,16], two-dimensional analysis [11–14,16,17], and constant interceptor and target speeds [11–14,16]. Solving the one-sided optimal control problem numerically, using methods such as steepest descent [10,15], can be done on more realistic models, but does not produce a general evasion strategy as with analytical studies. Unfortunately, perfect information on the missile's guidance law, parameters, and states, which are required for the application of these evasion guidance laws, are seldom available. Therefore, a separate identification scheme and estimator have to be constructed to identify the missile's guidance law, parameters, and states.

The evasion guidance laws, in which perfect information is not assumed, were typically formulated against a PN-guided missile, using two-dimensional linearized models. Because the evader does not have information on the missile's states and initial conditions, the evader has to perform a random maneuver, and thus performance is guarantied only in some statistical manner. Two types of random maneuvers were suggested: random telegraph [18,19] and a periodic sine or square wave maneuver with a random phase, in a frequency that is matched to the interceptor's navigation gain and time constant [20–22]. It was shown that the periodical random phase maneuver is superior to random telegraph and its root-mean-square reaches approximately 60–80% of the optimal deterministic value [23]. Although this formulation does not use information on the interceptor's state and initial conditions, it still requires information on the interceptor's time constant and navigation gain.

It is therefore evident that to effectively employ both categories of interceptor evasion guidance laws it is, by the very least, required to either obtain intelligence on the interceptor's guidance law and parameters or to identify them during the engagement. There are typically intelligence uncertainties and the adversary might employ a few different missiles. Therefore, to achieve adequate performance some sort of identification should be performed during the engagement. Contrary to the extensive literature on target-evasion guidance laws, there is very scarce open literature on missile guidance law and parameter identification. In [24] an algorithm is presented for identifying the parameters of a PN missile, for the purpose of countermeasures employment. The solution involves identification of four parameters associated with the PN guidance law and missile parameters, using a maximum likelihood estimator. The drawback of the proposed approach is that it only addresses a PN-guided interceptor missile and assumes that the initial launch position of the missile is known. In [25] an adaptive receding horizon controller is presented for evasion from an unknown interceptor missile. The controller uses Bayesian inference to identify the missile's guidance law from a closed set of guidance laws and parameters and uses this information to guide the evading target. The limitation of this approach is the assumption of having perfect information on the missile's states, with only the guidance law and parameters being unknown.

Therefore, although there has been substantial work in the literature on target evasion, most of the research concentrated on PN-guided interceptor missiles, which leaves the strategies against other missile guidance laws lacking. Furthermore, the lack of appropriate guidance law and parameter identification solutions greatly reduces the utility of the available target-evasion guidance laws. When combined with the typical maneuver and agility advantage of interceptor missiles over target aircraft (which is particularly evident for large expensive unmanned aerial vehicles with limited maneuverability and for military and civilian transport manned aircraft), it seems that most modern guidance laws provide sufficient performance to intercept aircraft with good probability. To overcome this inherent advantage of the missile over the target some authors proposed using a defender missile to protect the target [26]. The defender missile can be specifically designed for this mission.

In [27] the kinematic relations of three bodies: missile, target, and defender around a collision course in the plane are studied. The derivation assumes a nonmaneuvering target, no saturation limits on the missile and the defender, ideal dynamics for both the missile and the defender, and perfect information of the missile about the target and the defender about the missile. A discrete dynamic game of a defender with perfect information about the missile and the target (a nonmaneuvering ship) and a missile with perfect information about the target and no information about the defender is solved in [28]. The problem is formulated assuming ideal dynamics and discrete state and control spaces and is solved in mixed strategies. A similar problem is solved in [29] using continuous dynamics and an imperfect-information zero-sum differential-game formulation. In [30] the three-body problem is solved as a linear quadratic two-person (team) zero-sum differential game. Perfect state information is assumed as well as knowledge by all players of the dynamic model used by all participants in the game. All of the above defender guidance laws have been derived assuming that the defender missile has perfect information about the missile's states and parameters, which is seldom the case in real scenarios. Therefore, as in the target-evasion case, a separate identification scheme and estimator have to be constructed to apply these guidance laws.

The multiple-model adaptive estimator (MMAE) approach was originally introduced by Magill [31] and reformulated to recursive form by Sims and Lainiotis [32]. The algorithm is based on the assumption that the estimated system model belongs to a closed set of possible models. The main idea is that a bank of Kalman filters (KF) are run in parallel, with each filter matching a different possible model. The estimation is a weighted sum of the estimations from each filter in the bank, and the weights represent the probability of each model being true based on the measurement history. The output of the MMAE can be used to drive a single controller. This approach was employed in [33,34] to model possible target maneuvers and electronic countermeasures strategies.

Another approach is multiple-model adaptive control (MMAC) [35,36]. In the MMAC configuration, the estimation of each elementary filter in the MMAE scheme is fed into a controller matched to the filter's specific model, and the control command is a weighted sum of the controls from each filter in the bank. Unlike the MMAE approach, the MMAC approach is heuristic, but seems to yield good performance when a controller can be matched to each possible model.

In this paper we propose a cooperative guidance strategy for a defender missile and a protected aerial target that is chased by an interceptor missile. A cooperative information-sharing estimator is also proposed. The estimator uses measurements from the defender and the target and is a nonlinear adaptation of a MMAE. Each model in the MMAE represents a possible guidance strategy and guidance parameters of the intercepting missile. For each such model an optimal matched defender's guidance law is derived and used. Cooperation in guidance stems from the fact that the defender knows the evasive maneuvers to be performed by the protected target and thus the maneuvers it will induce on the incoming homing missile can be anticipated. Moreover, the target performs such a maneuver that minimizes the control effort requirements from the defender missile. The estimator, defender guidance law, and target-evasion law are joined in a MMAC configuration.

The remainder of this paper is organized as follows. The next section presents the mathematical models of the target–missile–defender (TMD) guidance and estimation problem, from the defender's perspective. The defender's information-sharing extended KF (EKF)-based MMAE is presented in Sec. III, followed by the derivation of a matched optimal control guidance law and MMAC scheme in Sec. IV. A comprehensive performance analysis of the proposed cooperative estimator and matched cooperative guidance law is presented in Sec. V, followed by concluding remarks.

II. Mathematical Model

We consider a scenario in which there are three bodies: a target aircraft, an intercepting missile, and a defender missile. For brevity, in the rest of the paper, we will refer to the target aircraft, the intercepting missile, and the defender missile as target, missile, and defender, respectively. This section presents the dynamics and measurement models of the estimation and guidance problem from the defender's perspective and addresses the assumptions taken in their derivation.

A. Nonlinear Kinematics and Dynamics

We consider skid-to-turn roll-stabilized missile and defender. The motion of the three bodies is assumed to transpire in the same plane. In Fig. 1 a schematic view of the planar endgame geometry is shown, where $X_I - O_I - Y_I$ is a Cartesian inertial reference frame. We denote variables associated with the target, missile, and defender by the subscripts t, m, and d, respectively. The speed, normal acceleration, and flight-path angles are denoted by V, a, and γ, respectively. The target–missile and defender–missile ranges are ρ_{tm} and ρ_{dm}, respectively; and λ_{tm} and λ_{dm} are target–missile and defender–missile line-of-sight (LOS) angles, respectively.

We assume that the target's and defender's own inertial state vectors

$$\boldsymbol{x}_i^I = [x_i \quad y_i \quad \gamma_i \quad a_i]^T, \qquad i \in \{t, d\} \tag{1}$$

are known to a very high accuracy (via some navigation system) and that the target can transmit its state vector to the defender without any delays.

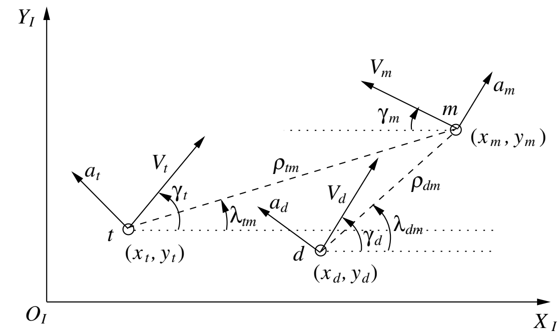

Fig. 1 Planar engagement geometry.

Remark 1. Only the relative position between the target and defender will be important in the rest of the derivation. Therefore, even if the absolute position states are not accurate, as long as the target is tracking the defender accurately the breakdown of this assumption will not invalidate the formulation and results presented in this paper.

The missile's acceleration command depends on the relative states between the missile and the target (via the missile's guidance law). For simplicity, we will assume in this paper that the missile has perfect information about the target. The missile's state vector of the target, in polar coordinates, is

$$\boldsymbol{x}_{tm}^R = [\rho_{tm} \quad \lambda_{tm} \quad \gamma_t \quad a_t]^T \tag{2}$$

We assume first-order lateral maneuver dynamics for the target and a constant target speed V_t. Therefore, the equations of motion (EOM) are

$$\dot{\rho}_{tm} = V_{\rho tm} \tag{3a}$$

$$\dot{\lambda}_{tm} = V_{\lambda tm}/\rho_{tm} \tag{3b}$$

$$\dot{\gamma}_t = a_t/V_t \tag{3c}$$

$$\dot{a}_t = (u_t - a_t)/\tau_t \tag{3d}$$

where

$$V_{\rho tm} = -[V_t \cos(\gamma_t - \lambda_{tm}) + V_m \cos(\gamma_m + \lambda_{tm})] \tag{4a}$$

$$V_{\lambda tm} = -V_t \sin(\gamma_t - \lambda_{tm}) + V_m \sin(\gamma_m + \lambda_{tm}) \tag{4b}$$

τ_t is the time constant of the target dynamics; u_t is the target's acceleration command; and V_t, τ_t, and u_t are assumed to be known or transmitted to the defender.

The defender's state vector of the missile in polar coordinates is

$$\boldsymbol{x}_{dm}^R = [\rho_{dm} \quad \lambda_{dm} \quad \gamma_m \quad a_m \quad V_m]^T \tag{5}$$

which we will represent as $\boldsymbol{x}$ in the rest of the paper to avoid excessive indexing.

We assume first-order lateral maneuver dynamics for the missile. We also assume that the missile moves at a constant speed V_m. Using these assumptions the EOM are

$$\dot{\rho}_{dm} = V_{\rho dm} \tag{6a}$$

$$\dot{\lambda}_{dm} = V_{\lambda dm}/\rho_{dm} \tag{6b}$$

$$\dot{\gamma}_m = a_m/V_m \tag{6c}$$

$$\dot{a}_m = (u_m(r, \boldsymbol{x}_{tm}^R) - a_m)/\tau_m \tag{6d}$$

$$\dot{V}_m = 0 \tag{6e}$$

where

$$V_{\rho dm} = -[V_d \cos(\gamma_d - \lambda_{dm}) + V_m \cos(\gamma_m + \lambda_{dm})] \tag{7a}$$

$$V_{\lambda dm} = -V_d \sin(\gamma_d - \lambda_{dm}) + V_m \sin(\gamma_m + \lambda_{dm}) \tag{7b}$$

τ_m is the time constant of the missile dynamics, and $u_m(r, \boldsymbol{x}^R_{tm})$ is the missile's acceleration command. We assume that the missile has no information on the defender, it is not trying to evade the defender, and it is guided to the target via one of a closed set of guidance laws and guidance parameters, which we will refer to as the regime $r \in \{1, \ldots, s\}$. Each such regime will generate different missile acceleration commands u_m and will therefore result in different missile trajectories.

Remark 2. These are very realistic assumptions, as most missiles can only track a single target, are only designed to intercept the tracked target, and some intelligence is typically available on the adversaries missiles, which facilitates discretization to a closed set of options.

Remark 3. In this formulation we assume for simplicity that τ_m is a known parameter. If this is not the case we can address the uncertainty in two ways. We can represent different values of τ_m as different regimes and address the problem in the same way we address the guidance law uncertainty or we can add it as a constant state in Eq. (6).

The discrete-time version of the EOM (6) can be generally described as

$$\boldsymbol{x}_k = \mathbf{f}_{k-1}(\boldsymbol{x}_{k-1}, r, \boldsymbol{x}^R_{tm}) \tag{8}$$

where $\boldsymbol{x}_k$ is the relative state vector $\boldsymbol{x}^R_{dm}$ at time t_k, $\mathbf{f}_{k-1}$ is derived by integrating Eqs. (6) from t_{k-1} to t_k, and r is the regime.

We assume that the defender's dynamics during the endgame can be represented by arbitrary order linear equations:

$$\dot{\boldsymbol{y}}_d = \mathbf{A}_d \boldsymbol{y}_d + \mathbf{B}_d u_d \tag{9a}$$

$$\dot{\gamma}_d = a_d / V_d \tag{9b}$$

where

$$a_d = \mathbf{C}_d \boldsymbol{y}_d + D_d u_d \tag{10}$$

and $\boldsymbol{y}_d$ is the state vector of the defender's internal state variables with $\dim(\boldsymbol{y}_d) = n$. We denote the part of the acceleration without dynamics, if it exists, as the direct lift and the part with dynamics as the specific force.

B. Linearized Kinematics for Defender Guidance Law Derivation

We derive the defender guidance law based on a linearized model. If during the endgame the defender and missile deviations from the collision triangle are small, then the linearization is justified. In Fig. 2 a schematic view of the linearized planar endgame geometry is shown. The X axis, aligned with the LOS used for linearization, is denoted as LOS_0, and ξ is the relative displacement between the defender and the missile normal to this direction. The defender and missile accelerations normal to LOS_0 are denoted by a^n_d and a^n_m, respectively, and satisfy $a^n_d = a_d \cos(\gamma_{d0} - \lambda_{dm0})$ and $a^n_m = a_m \cos(\gamma_{m0} + \lambda_{dm0})$.

The state vector of the linearized guidance problem is

$$\boldsymbol{y} = [\xi \quad \dot{\xi} \quad \boldsymbol{y}^T_d]^T \tag{11}$$

The equations of motion are

$$\dot{\boldsymbol{y}} = \begin{cases} \dot{y}_1 = y_2 \\ \dot{y}_2 = a_m \cos(\gamma_{m0} + \lambda_{dm0}) - a_d \cos(\gamma_{d0} - \lambda_{dm0}) \\ \dot{\boldsymbol{y}}_d = \mathbf{A}_d \boldsymbol{y}_d + \mathbf{B}_d u_d \end{cases} \tag{12}$$

The matrix form of the equation set is therefore

$$\dot{\boldsymbol{y}} = \mathbf{A}\boldsymbol{y} + \mathbf{B}u_d + \mathbf{C}a_m \tag{13}$$

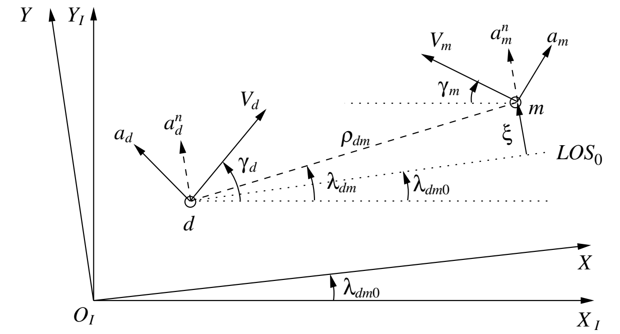

Fig. 2 Linearized planar engagement geometry.

where

$$\mathbf{A} = \begin{bmatrix} 0 & 1 & [0]_{1\times n} \\ 0 & 0 & -\mathbf{C}_d \cos(\gamma_{d0} - \lambda_{dm0}) \\ 0 & 0 & \mathbf{A}_d \end{bmatrix}$$

$$\mathbf{B} = \begin{bmatrix} 0 \\ -D_d \cos(\gamma_{d0} - \lambda_{dm0}) \\ \mathbf{B}_d \end{bmatrix}, \qquad \mathbf{C} = \begin{bmatrix} 0 \\ \cos(\gamma_{m0} + \lambda_{dm0}) \\ 0 \end{bmatrix} \tag{14}$$

with [0] denoting a matrix of zeros with appropriate dimensions.

Once a collision triangle is reached and maintained, the speed $V_{\rho dm}$ is constant and the defender–missile interception time can be approximated by

$$t^{dm}_f = -\rho_{dm0} / V_{\rho dm0} \tag{15}$$

C. Measurement Model

The target and the defender are assumed to be equipped with either radar or electro-optic sensors. Therefore, each one may acquire: both ρ_i and λ_i measurements or only λ_i, where $i \in \{dm, tm\}$. The measurements are assumed to be contaminated by a zero-mean white Gaussian measurement noise, $\boldsymbol{v}_k$. All of the measurements are assumed to be mutually independent. Therefore, the measurement model when the target and defender cooperate (share information) and when all possible measurements are available is

$$\boldsymbol{z}_k = \mathbf{h}_k(\boldsymbol{x}_k) + \boldsymbol{v}_k = \begin{bmatrix} \rho_{dm}(k) \\ \lambda_{dm}(k) \\ \rho_{tm}(k) \\ \lambda_{tm}(k) \end{bmatrix} + \boldsymbol{v}_k$$

$$= \begin{bmatrix} \rho_{dm}(k) \\ \lambda_{dm}(k) \\ \sqrt{(\Delta X^2_{tm} + \Delta Y^2_{tm})} \\ \arctan(\Delta Y_{tm} / \Delta X_{tm}) \end{bmatrix} + \boldsymbol{v}_k \tag{16}$$

where

$$\Delta X_{tm} = \Delta X_{td} + \rho_{dm}(k) \cos[\lambda_{dm}(k)], \qquad \Delta X_{td} = x_d(k) - x_t(k) \tag{17a}$$

$$\Delta Y_{tm} = \Delta Y_{td} + \rho_{dm}(k) \sin[\lambda_{dm}(k)], \qquad \Delta Y_{td} = y_d(k) - y_t(k) \tag{17b}$$

and

$$\boldsymbol{v}_k \sim \mathcal{N}([0]_{4\times 1}, \mathbf{R}), \qquad \mathbf{R} = \mathrm{diag}\{\sigma^2_{\rho dm}, \sigma^2_{\lambda dm}, \sigma^2_{\rho tm}, \sigma^2_{\lambda tm}\} \tag{18}$$

When the defender and target do not cooperate, the target does not transmit any measurements to the defender and hence the defender's measurement model degenerates to

$$z_k = \mathbf{h}_k(\boldsymbol{x}_k) + \boldsymbol{v}_k = \begin{bmatrix} \rho_{dm}(k) \\ \lambda_{dm}(k) \end{bmatrix} + \boldsymbol{v}_k, \qquad \boldsymbol{v}_k \sim \mathcal{N}([0]_{2\times 1}, \mathbf{R}) \qquad (19)$$
$$\mathbf{R} = \mathrm{diag}\{\sigma^2_{\rho dm}, \sigma^2_{\lambda dm}\}$$

If ρ_i, for $i \in \{dm, tm\}$, is not available (due to sensor type), the appropriate row is eliminated from $\mathbf{h}_k$ and the appropriate row and column are eliminated from $\mathbf{R}$.

III. MMAE for Missile Tracking and Identification

The MMAE is a well-known approach for estimation with model uncertainty [31,32,37]. In this section we first present the MMAE algorithm, followed by a derivation of a specific EKF-based MMAE for estimating the missile's state vector and identification of its guidance law and guidance law parameters.

A. Multiple-Model Adaptive Estimator

The MMAE, also known as the static multiple-model estimator [37], was designed to estimate dynamic models with parametric uncertainty, such as the missile model presented in Sec. II [see Eqs. (6)]. The MMAE addresses a scenario in which the system dynamics has a known finite set of possible regimes and in which the true system regime is fixed during the entire measurement history (no switching between regimes). The main idea is that a bank of KFs (or EKFs in the nonlinear case) are run in parallel, with each filter matching a different possible regime. The estimation is a weighted sum of the estimations from each filter in the bank, and the weights represent the probability of each regime being correct based on the measurement history. The regime probabilities at each time step are calculated based on Bayesian inference, using the previous time step's regime probabilities and the regime-conditioned likelihood of the new measurement. We next present the mathematical formulation of the generic MMAE algorithm.

Let $\mathcal{Z}_{k-1} \triangleq \{z_i; i = 1, \ldots, k-1\}$ be the measurement history up to time $k-1$, and let $\mu^j_{k-1} = Pr\{r = j|\mathcal{Z}_{k-1}\}$ be the posterior probability at $k-1$ that the jth regime is correct. Using Bayes's rule, the posterior probability at time k that the jth regime is correct equals

$$\mu^j_k = Pr\{r = j|\mathcal{Z}_k\} = \frac{p(z_k|r = j, \mathcal{Z}_{k-1})\mu^j_{k-1}}{p(z_k|\mathcal{Z}_{k-1})} \qquad (20)$$

Applying the total probability theorem to the denominator yields

$$\mu^j_k = \frac{\Lambda^j_k \mu^j_{k-1}}{\sum_{i=1}^s \Lambda^i_k \mu^i_{k-1}} \qquad (21)$$

where $\Lambda^j_k = p(z_k|r = j, \mathcal{Z}_{k-1})$ is the jth-regime-conditioned likelihood function, which is calculated using the jth filter innovations process statistics. Under the linear-Gaussian assumptions, Λ^j_k is Gaussian and is given by

$$\Lambda^j_k \sim \mathcal{N}(\nu^j_k; 0, \mathbf{S}^j_k) \qquad (22)$$

where ν^j_k and $\mathbf{S}^j_k$ are the innovation and its covariance from the jth-regime-matched filter. In the nonlinear or non-Gaussian cases, Eq. (22) is still used, although it is only an approximation. Thus, a KF (or EKF) is constructed for each regime, yielding a regime-conditioned state estimate $\hat{\boldsymbol{x}}^j_{k|k}$ and a regime-conditioned covariance matrix $\mathbf{P}^j_{k|k}$. The estimates and covariances from each filter in the bank are blended according to each regime's probability of being correct [Eq. (21)], yielding

$$\hat{\boldsymbol{x}}_{k|k} = \sum_{j=1}^s \hat{\boldsymbol{x}}^j_{k|k}\mu^j_k \qquad (23a)$$

$$\mathbf{P}_{k|k} = \sum_{j=1}^s \mu^j_k\{\mathbf{P}^j_{k|k} + [\hat{\boldsymbol{x}}^j_{k|k} - \hat{\boldsymbol{x}}_{k|k}][\hat{\boldsymbol{x}}^j_{k|k} - \hat{\boldsymbol{x}}_{k|k}]^T\} \qquad (23b)$$

Figure 3 presents the schematic structure of a generic MMAE for two regimes.

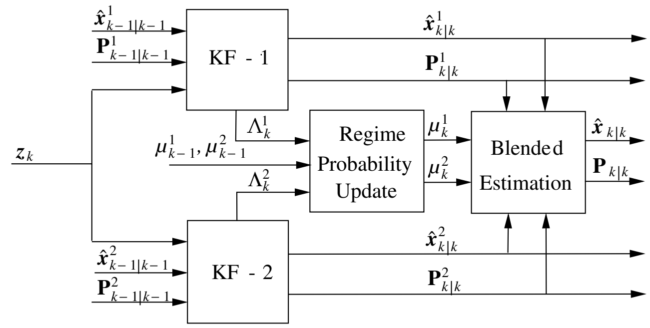

Fig. 3 Generic MMAE for two regimes.

B. Missile Tracking and Identification Filter

The missile-tracking EKF-based MMAE proposed in this paper is based on the generic MMAE algorithm presented in the previous subsection, adapted to the models formulated in Sec. II. In our case the regimes represent different guidance laws and guidance parameters of the missile. Therefore, in Eq. (6), each regime incorporates a different $u_m(r, \boldsymbol{x}^R_{tm})$. As our model is nonlinear an EKF regime-matched filter is derived.

Remark 4. We assume that the missile is guided to the target via one fixed guidance law (i.e. the missile does not switch between guidance laws during the engagement). Although this is a very realistic assumption for the endgame, if this assumption does not hold a similar estimator can be derived based on the interacting-multiple-model (IMM) [37] approach. The IMM allows transitions between regimes, but the transition probabilities between regimes are required.

The propagated state from time $k-1$ to time k, $\hat{\boldsymbol{x}}^j_{k|k-1}$ is calculated via integration of Eqs. (6), using the appropriate u_m for each regime. For simplicity, we will limit the derivation in this paper to three representative missile guidance laws: PN, APN, and OGL. The derivation can be extended to other missile guidance laws using the same formulation and similar derivation steps.

1. *Set of Missile Guidance Laws*

The missile guidance law in each regime has the following form:

$$u^j_m = \frac{N'_j Z_j}{(t^{tm}_{\mathrm{go}})^2 \cos(\gamma_m + \lambda_{tm})}; \qquad j = 1\ldots, s \qquad (24)$$

where t^{tm}_{go} can be approximated for every filter by

$$t^{tm}_{\mathrm{go}} = -\rho_{tm}/V_{\rho tm} \qquad (25)$$

The zero-effort miss (ZEM) associated with each guidance law is one of the following:

$$Z_{\mathrm{PN}} = V_{\rho tm}(t^{tm}_{\mathrm{go}})^2\dot{\lambda}_{tm} \qquad (26a)$$

$$Z_{\mathrm{APN}} = Z_{\mathrm{PN}} + \frac{(t^{tm}_{\mathrm{go}})^2}{2} a_t \cos(\gamma_t - \lambda_{tm}) \qquad (26b)$$

$$Z_{\mathrm{OGL}} = Z_{\mathrm{APN}} - \tau^2_m \psi(\theta) a_m \cos(\gamma_m + \lambda_{tm}) \qquad (26c)$$

where

$$\psi(\theta) = \exp(-\theta) + \theta - 1 \qquad (27)$$

θ is the normalized time-to-go,

$$\theta = t^{tm}_{\mathrm{go}}/\tau_m \qquad (28)$$

λ_{tm} and ρ_{tm} are

$$\lambda_{tm} = \arctan(\Delta Y_{tm}/\Delta X_{tm}), \qquad \rho_{tm} = \sqrt{(\Delta X^2_{tm} + \Delta Y^2_{tm})} \qquad (29)$$

and $\dot{\lambda}_{tm}$ and $V_{\rho tm}$ are given by Eqs. (3) and (4), respectively.

The navigation gains of PN and APN (N'_{PN} and N'_{APN}, respectively) are constant, whereas that of OGL is time-varying:

$$N'_{\mathrm{OGL}} = \frac{6\theta^2\psi(\theta)}{3 + 6\theta - 6\theta^2 + 2\theta^3 - 3e^{-2\theta} - 12\theta e^{-\theta} + 6\alpha/\tau_m^3} \tag{30}$$

where α represents the ratio between the weight on the control effort (integral of the acceleration command squared) and the miss distance in the quadratic cost function used in the OGL formulation:

$$J_m = \frac{a}{2}(\mathrm{miss})^2 + \frac{1}{2}\int_0^{t_f^{tm}} [u_m \cos(\gamma_{m0} + \lambda_{tm0})]^2\,\mathrm{d}t, \qquad \alpha \triangleq 1/a \tag{31}$$

Identifying the missile guidance law requires the identification of the ZEM (either Z_{PN}, Z_{APN}, or Z_{OGL}) and navigation gain (either N'_{PN}, N'_{APN}, or N'_{OGL}). With regard to the navigation gain, in the case of PN and APN the requirement it to identify its constant value, whereas for OGL the requirement is to identify α.

When the defender and target do not cooperate, the target does not transmit any measurements to the defender and the defender's measurement Jacobian matrix degenerates to

$$\mathbf{H}_x^j = \begin{bmatrix} 1 & 0 & 0 & 0 & 0 \\ 0 & 1 & 0 & 0 & 0 \end{bmatrix} \tag{37}$$

If the measurement ρ_i, for $i \in \{dm, tm\}$, is not available (due to sensor type) the appropriate row is eliminated from $\mathbf{H}_x^j$ and the appropriate row and column are eliminated from $\mathbf{R}$.

The updated covariance matrix is calculated using the Joseph formula,

$$\mathbf{P}_{k|k}^j = [\mathbf{I} - \mathbf{K}_k^j\mathbf{H}_x^j]\mathbf{P}_{k|k-1}^j[\mathbf{I} - \mathbf{K}_k^j\mathbf{H}_x^j]^T + \mathbf{K}_k^j\mathbf{R}[\mathbf{K}_k^j]^T \tag{38}$$

2. Prediction and Measurement Update

The Jacobian matrix associated with the dynamics of Eq. (6) is

$$\mathbf{F}_x^j = \left.\begin{bmatrix} 0 & V_{\lambda dm} & V_m \sin(\gamma_m + \lambda_{dm}) & 0 & -\cos(\gamma_m + \lambda_{dm}) \\ \frac{-V_{\lambda dm}}{\rho_{dm}^2} & \frac{-V_{\rho dm}}{\rho_{dm}} & \frac{V_m \cos(\gamma_m+\lambda_{dm})}{\rho_{dm}} & 0 & \frac{\sin(\gamma_m+\lambda_{dm})}{\rho_{dm}} \\ 0 & 0 & 0 & \frac{1}{V_m} & -\frac{a_m}{V_m^2} \\ \frac{1}{\tau_m}\frac{\partial u_m^j}{\partial \rho_{dm}} & \frac{1}{\tau_m}\frac{\partial u_m^j}{\partial \lambda_{dm}} & \frac{1}{\tau_m}\frac{\partial u_m^j}{\partial \gamma_m} & \frac{1}{\tau_m}\left(\frac{\partial u_m^j}{\partial a_m} - 1\right) & \frac{1}{\tau_m}\frac{\partial u_m^j}{\partial V_m} \\ 0 & 0 & 0 & 0 & 0 \end{bmatrix}\right|_{x=\hat{x}^j_{(k-1|k-1)}} \tag{32}$$

where the partial derivatives of u_m^j with respect to the states for the considered missile guidance laws are presented in the Appendix.

The prediction error covariance matrix of the filter matched to the jth regime is

$$\begin{gathered} \mathbf{P}_{k|k-1}^j = \mathbf{\Phi}(k, k-1)\mathbf{P}_{k-1|k-1}^j\mathbf{\Phi}^T(k, k-1) + \mathbf{Q}_d \\ \mathbf{\Phi}(k, k-1) = e^{\mathbf{F}_x^j T} \end{gathered} \tag{33}$$

where $\mathbf{\Phi}(k, k-1)$ is the transition matrix associated with the system dynamics, assuming that $\mathbf{F}_x^j$ is fixed during the interval $(t_{k-1}, t_k]$, $T = t_k - t_{k-1}$ is the sampling time, and $\mathbf{Q}_d$ is the covariance matrix of the equivalent discrete process noise, used as a tuning matrix.

The updated state estimate of the filter matched to the jth regime is

$$\hat{\boldsymbol{x}}_{k|k}^j = \hat{\boldsymbol{x}}_{k|k-1}^j + \mathbf{K}_k^j[z_k - \mathbf{h}_k(\hat{\boldsymbol{x}}_{k|k-1}^j)] \tag{34}$$

where $\mathbf{K}_k^j$ is the Kalman gain, computed as

$$\mathbf{K}_k^j = \mathbf{P}_{k|k-1}^j[\mathbf{H}_x^j]^T[\mathbf{S}_k^j]^{-1} \tag{35a}$$

$$\mathbf{S}_k^j = \mathbf{H}_x^j\mathbf{P}_{k|k-1}^j[\mathbf{H}_x^j]^T + \mathbf{R} \tag{35b}$$

$\mathbf{S}_k^j$ is the covariance of the innovations process, $\mathbf{R}$ is the measurement noise covariance matrix, and $\mathbf{H}_x^j$ is the measurement Jacobian matrix, associated with the measurement model of Eq. (16):

$$\begin{aligned} \mathbf{H}_x^j &= \left.\begin{bmatrix} 1 & 0 & 0 & 0 & 0 \\ 0 & 1 & 0 & 0 & 0 \\ \frac{\partial \rho_{tm}}{\partial \rho_{dm}} & \frac{\partial \rho_{tm}}{\partial \lambda_{dm}} & 0 & 0 & 0 \\ \frac{\partial \lambda_{tm}}{\partial \rho_{dm}} & \frac{\partial \lambda_{tm}}{\partial \lambda_{dm}} & 0 & 0 & 0 \end{bmatrix}\right|_{x=\hat{x}^j_{(k|k-1)}} \\ &= \left.\begin{bmatrix} 1 & 0 & 0 & 0 & 0 \\ 0 & 1 & 0 & 0 & 0 \\ \frac{\Delta_3}{\rho_{tm}} & -\frac{\rho_{dm}\Delta_2}{\rho_{tm}} & 0 & 0 & 0 \\ \frac{\Delta_2}{\rho_{tm}^2} & \frac{\rho_{dm}\Delta_3}{\rho_{tm}^2} & 0 & 0 & 0 \end{bmatrix}\right|_{x=\hat{x}^j_{(k|k-1)}} \end{aligned} \tag{36}$$

where Δ_2 and Δ_3 are defined in Eqs. (A7) and (A8).

and the mode conditioned likelihood Λ_k^j is calculated using the innovations process distribution:

$$\Lambda_k^j = p(z_k | r = j, \mathcal{Z}_{k-1}) \sim \mathcal{N}(z_k; \hat{z}_{k|k-1}^j, \mathbf{S}_k^j) \tag{39}$$

where $\hat{z}_{k|k-1}^j$ is the predicted measurement (computed by the filter).

IV. Cooperative Guidance

In this section we derive the cooperative defender–target OGL, matched to the missile's guidance law. It uses cooperation between the aerial target and the defender missile, which stems from the fact that the defender knows the evasive maneuvers to be performed by the protected target and thus can anticipate the maneuvers it will induce on the incoming homing missile. This guidance law is then used to construct a MMAC-based adaptive guidance law in which each elementary filter controller in the guidance scheme is matched to a possible guidance strategy (PN, APN, or OGL) and guidance parameters of the missile. In the next step we derive a bang–bang target maneuver matched to the missile's guidance law that minimizes the defender's control effort during the engagement. The matched target maneuver is then used to construct a MMAC-based adaptive guidance law for the target.

A. Cooperative Optimal Guidance Law

The quadratic cost function chosen for the cooperative optimal guidance law (COGL) is

$$J_c = \frac{b}{2}y_1^2(t_f^{dm}) + \frac{1}{2}\int_0^{t_f^{dm}} u^2\,\mathrm{d}t \tag{40}$$

where b is a nonnegative weight and

$$u = u_d \cos(\gamma_{d0} - \lambda_{dm0}) \tag{41}$$

is the projection of the defender's command in the direction perpendicular to LOS_0. Note that letting $b \to \infty$ yields a perfect-intercept requirement and that an integral cost on u^2 is a common representation of the control effort [1–3,5].

1. Order Reduction

Bryson and Ho [4] introduced a transformation enabling reducing a problem's order. This transformation is sometimes denoted as *terminal projection*. We will use a similar transformation [38]. Let us define a new state $Z_{dm}(t)$ that satisfies

$$Z_{dm}(t) = \mathbf{D}\mathbf{\Phi}(t_f^{dm}, t)\boldsymbol{y}(t) + \mathbf{D}\int_t^{t_f^{dm}} \mathbf{\Phi}(t_f^{dm}, \tau)\mathbf{C}a_m(\tau)\,\mathrm{d}\tau \tag{42}$$

where $\mathbf{\Phi}(t_f^{dm}, t)$ is the transition matrix associated with Eq. (13), and $\mathbf{D}$ is a constant vector:

$$\mathbf{D} = [\,1 \quad 0 \quad [0]_{1\times n}\,] \tag{43}$$

Then the derivative with respect to time of the new state $Z_{dm}(t)$ is

$$\begin{aligned}\dot{Z}_{dm} &= \mathbf{D}[\dot{\mathbf{\Phi}}(t_f^{dm}, t)\boldsymbol{y} + \mathbf{\Phi}(t_f^{dm}, t)\dot{\boldsymbol{y}}] - \mathbf{D}\mathbf{\Phi}(t_f^{dm}, t)\mathbf{C}a_m \\ &= \mathbf{D}\mathbf{\Phi}(t_f^{dm}, t)\mathbf{B}u_d\end{aligned} \tag{44}$$

which is state-independent. $Z_{dm}(t_f^{dm})$ can be expressed using Eq. (42) as

$$Z_{dm}(t_f^{dm}) = \mathbf{D}\boldsymbol{y}(t_f^{dm}) = y_1(t_f^{dm}) \tag{45}$$

Using this new variable, the cost function from Eq. (40) can also be expressed using only the new state $Z_{dm}(t)$ as

$$J_c = \frac{b}{2}Z_{dm}^2(t_f^{dm}) + \frac{1}{2}\int_0^{t_f^{dm}} u^2\,\mathrm{d}t \tag{46}$$

Remark 5. In addition to reducing the order of the problem, the new state $Z_{dm}(t)$ has an important physical meaning. $Z_{dm}(t)$ is known as the zero-effort miss, which is the miss distance if from the current time onward the defender will not apply any control and the missile will perform its assumed maneuver. We assume the defender and target cooperate; therefore, the defender knows the future maneuver strategy of the target. Given a missile guidance law, this information can be used to obtain a_m as a function of time via integration of Eqs. (3) and (6).

2. Optimal Controller

The Hamiltonian of the problem is

$$H = \tfrac{1}{2}u^2 + \lambda_z\dot{Z}_{dm} \tag{47}$$

The adjoint equation and solution is

$$\begin{aligned}&\dot{\lambda}_z = -\frac{\partial H}{\partial Z_{dm}} = 0; \\ &\lambda_z(t_f^{dm}) = bZ_{dm}(t_f^{dm}) \Rightarrow \lambda_z(t) = bZ_{dm}(t_f^{dm})\end{aligned} \tag{48}$$

The optimal controller for the defender satisfies $u^* = \arg_u \min H$.

For obtaining an analytic solution for the guidance law u^*, we will assume the defender has first-order dynamics with a time constant of τ_d. In which case the matrices of Eqs. (9) and (10) degenerate to $\mathbf{A}_d = -1/\tau_d$, $\mathbf{B}_d = 1/\tau_d$, $\mathbf{C}_d = 1$, and $D_d = 0$, and the dynamic equation of Z_{dm} [Eq. (44)] simplifies to

$$\dot{Z}_{dm} = -\tau_d\psi(\eta)u \tag{49}$$

where

$$\eta = t_{\mathrm{go}}^{dm}/\tau_d \tag{50}$$

is the normalized time-to-go in the defender–missile interception, ψ is given by Eq. (27), and t_{go}^{dm} can be approximated by

$$t_{\mathrm{go}}^{dm} = -\rho_{dm}/V_{\rho dm} \tag{51}$$

For the considered first-order defender dynamics, the optimal guidance law simplifies to

$$\frac{\partial H}{\partial u} = 0 \Rightarrow u^*(t) = \lambda_z(t)\tau_d\psi(\eta) = bZ_{dm}(t_f^{dm})\tau_d\psi(\eta) \tag{52}$$

Substituting Eq. (52) into Eq. (49) and integrating from t to t_f^{dm}, using the end conditions from Eq. (45) yields

$$Z_{dm}(t_f^{dm}) = \frac{Z_{dm}(t)}{1 + b\tau_d^2 g(t)} \tag{53}$$

where

$$\begin{aligned}g(t) &= \int_t^{t_f^{dm}} \psi^2\left(\frac{t_f^{dm} - \tau}{\tau_d}\right)\mathrm{d}\tau = \tau_d\int_0^{\eta}\psi^2(\xi)\,\mathrm{d}\xi \\ &= \frac{\tau_d}{6}(2\eta^3 - 6\eta^2 + 6\eta + 3 - 12\eta e^{-\eta} - 3e^{-2\eta})\end{aligned} \tag{54}$$

Substituting Eq. (53) into Eq. (52) yields the following optimal controller:

$$u^*(t) = \frac{N'_{\mathrm{COGL}}Z_{dm}(t)}{(t_{\mathrm{go}}^{dm})^2} \tag{55}$$

where

$$\begin{aligned}Z_{dm}(t) &= y_1 + y_2t_{\mathrm{go}}^{dm} - \tau_d^2\psi(\eta)a_d\cos(\gamma_{d0} - \lambda_{dm0}) \\ &\quad + \int_t^{t_f^{dm}} t_{\mathrm{go}}^{dm}a_m(\tau)\cos(\gamma_{m0} + \lambda_{dm0})\,\mathrm{d}\tau\end{aligned} \tag{56}$$

and

$$N'_{\mathrm{COGL}} = \frac{6\eta^2\psi(\eta)}{3 + 6\eta - 6\eta^2 + 2\eta^3 - 3e^{-2\eta} - 12\eta e^{-\eta} + \frac{6\beta}{\tau_d^3}}, \qquad \beta \triangleq 1/b \tag{57}$$

By using the small deviation from collision triangle assumption, the displacement ξ normal to the initial LOS can be approximated by

$$\xi \approx (\lambda_{dm} - \lambda_{dm0})\rho_{dm} \tag{58}$$

Differentiating Eq. (58) with respect to time yields

$$y_1 + y_2t_{\mathrm{go}}^{dm} = \xi + \dot{\xi}t_{\mathrm{go}}^{dm} \approx -V_{\rho dm}(t_{\mathrm{go}}^{dm})^2\dot{\lambda}_{dm} \tag{59}$$

Therefore, $Z_{dm}(t)$ of Eq. (56) can be expressed as

$$\begin{aligned}Z_{dm}(t) &= -V_{\rho dm}(t_{\mathrm{go}}^{dm})^2\dot{\lambda}_{dm} - \tau_d^2\psi(\eta)a_d\cos(\gamma_{d0} - \lambda_{dm0}) \\ &\quad + \int_t^{t_f^{dm}} t_{\mathrm{go}}^{dm}a_m(\tau)\cos(\gamma_{m0} + \lambda_{dm0})\,\mathrm{d}\tau\end{aligned} \tag{60}$$

where all components of $Z_{dm}(t)$ are either directly estimated or can be calculated using the outputs of the estimator derived in Sec. III. The integral component of the Z_{dm} is evaluated by numerical integration of Eqs. (3) and (6), using a fourth-order Runge–Kutta algorithm. The integration is performed using a constant number of integration steps from t to t_f^{dm}. Consequently, the computation burden at each time step is equal and the integration resolution improves as the defender and missile approach each other.

Remark 6. If a_m is assumed fixed the COGL of Eqs. (55–57) degenerates to the OGL presented in [3].

Remark 7. A possible method to improve performance, known as predictive guidance [1], is to evaluate Z_{dm} using simulation. This is performed by running a simulation from t to t_f^{dm} at each time step with a nulled defender command u_d and the assumed missile acceleration a_m. By definition, Z_{dm} is the miss distance obtained in this simulation. This approach yields a more accurate computation of the ZEM, which can be employed in Eq. (55). However, it requires substantially larger computational power and thus was not used in this paper.

B. MMAC Guidance Law

Thus far, we have derived a defender guidance law assuming the missile's acceleration until the end of the engagement is known. Unfortunately, this is typically not the case. However, we can exploit the fact that the missile is trying to intercept the target. By assuming that the missile's guidance law belongs to a closed set of guidance laws (see Sec. III.B, Eq. (24)) and the defender's knowledge of the target's strategy, we can derive a MMAC guidance law in which each filter controller is matched to a possible missile guidance strategy and parameters.

In the MMAC approach [35,36] the estimation of each elementary filter in the MMAE scheme, presented in Sec. III.A, is fed into a controller matched to the filter's specific regime, and the control command is a weighted sum of the controls from each filter controller in the bank. The weighting of each filter controller is its posterior probability based on the measurement history. The control command at time k (u_k) can therefore be calculated as

$$u_k = \sum_{j=1}^{s} \mu_k^j u_k^j = \sum_{j=1}^{s} \mu_k^j \frac{N'^j_{\mathrm{COGL}} Z^j_{dm}}{(t_{\mathrm{go}}^{dmj})^2} \tag{61}$$

where u_k^j represents the controller associated with the jth regime.

Assuming that the computation of t_{go}^{dm} is almost identical for all models, the difference between the control commands in the different regimes lies in the computation of Z_{dm}, based on Eq. (60). Thus, we can write

$$u_k \approx \frac{N'_{\mathrm{COGL}}}{(t_{\mathrm{go}}^{dm})^2} \sum_{j=1}^{s} \mu_k^j Z^j_{dm} \tag{62}$$

Figure 4 presents the schematic structure of a generic MMAC for two regimes.

Unlike the MMAE approach, the MMAC approach is heuristic (an approximation), but seems to yield good performance when a controller can be matched to each possible regime.

This framework perfectly fits our target–missile–defender problem. As each regime in the MMAE of Sec. III.B corresponds to a known missile guidance strategy and guidance parameters, we can derive the missile acceleration a_m given this information and employ the defender guidance law derived in Sec. IV.A on the estimations of each elementary filter. Using this scheme, as the identification of the missile's guidance law and parameters improves during the engagement, the defender's guidance law will adapt to fit the identified missile's guidance law.

Remark 8. In the derivation of the defender MMAC guidance law it was assumed that the defender has information on the future maneuver strategy of the target. This assumption requires the target to follow the evasive maneuver communicated to the defender, after the defender has been launched. For a manned aircraft this implies that the pilot follows the evasive maneuver, which can be accomplished either by generating evasion flight directions for the pilot to follow, or some sort of autoevasion autopilot. For an unmanned aerial vehicle (UAV), an autoevasion autopilot is the natural solution, as we would like the UAV to be autonomous and require minimal human intervention.

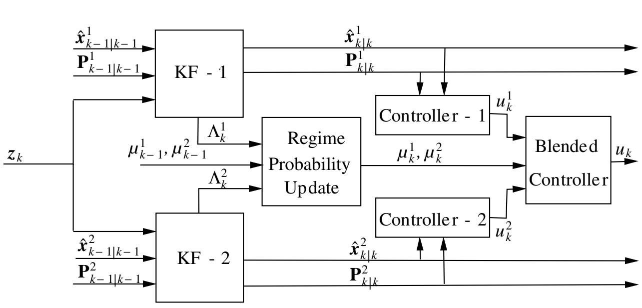

Fig. 4 Generic MMAC for two regimes.

C. Minimizing Defender Control Effort

The derivation above is general and valid for any target-evasion strategy. The only requirement is that the target strategy must be known to the defender missile. This target strategy may be, for example, the optimal (in some sense) evasion maneuver (such as the strategies described in Sec. I) or a strategy derived so as to enable quick discrimination between the different missile guidance laws.

For a bang–bang target maneuver and a given missile guidance law, we can minimize the defender's control effort by choosing a target switch time t_{sw} that minimizes $|Z_{dm}|$ [Eq. (60)]. By definition, Z_{dm} is the zero-effort miss in the defender–missile engagement. Therefore, by choosing a switch time that minimizes $|Z_{dm}|$, we minimize $|u^*(t)|$ [Eq. (55)]. Furthermore, if there is a t_{sw} for which $Z_{dm} = 0$, then according to Eqs. (49) and (55), $u^*(t)$ will remain zero throughout the duration of the engagement. Calculating t_{sw} that minimizes $|Z_{dm}|$ can be performed numerically, using standard methods such as gradient decent. Because we assumed that the missile's guidance law belongs to a closed set of options, we propose to apply the MMAC approach to ascertain t_{sw},

$$t_{\mathrm{sw}} = \arg \min_{t_{\mathrm{sw}} \in [t_k, t_f]} \left[\sum_{j=1}^{s} \mu_k^j Z^j_{dm} \right] \tag{63}$$

or an approximation of this approach:

$$t_{\mathrm{sw}} \approx \sum_{j=1}^{s} \mu_k^j [\arg \min_{t^j_{\mathrm{sw}} \in [t_k, t_f]} Z^j_{dm}] \tag{64}$$

In the MMAC approach, as our confidence in the missile's guidance law improves, so does our assessment of the optimal target switch time. In the rest of this paper we will refer to the cooperative guidance law in which the defender performs MMAC-based COGL and the target performs a bang–bang maneuver at a switch time calculated via Eq. (64) as optimal-switch COGL (OSCOGL).

Remark 9. The update of the optimal-switch time is only required before the target switch transpires.

Remark 10. A possible way to reduce the computational effort is to calculate t_{sw} at a lower frequency than the measurement frequency or only calculate it at the beginning of the engagement. The practical benefit of fine tuning t_{sw} at each sample is relatively small, because the difference in t_{sw} for the evaluated missile guidance laws (PN, APN, and OGL) is typically small.

V. Performance Analysis

The performance of the missile-tracking MMAE and the defender's and target's adaptive cooperative guidance laws developed in this paper are evaluated in this section via simulation, using nonlinear kinematics and the target, missile, and defender dynamics. We first present the simulation environment and interception scenario, followed by a sample run. We then present a Monte Carlo (MC) simulation study demonstrating the performance of the proposed combined estimation and guidance MMAC schemes.

A. Simulation Environment and Scenario

The simulation includes a target, missile, and defender. The engagements are initiated at missile and target flight-path angles of $\gamma_{m0} \in [-30, 30]$ deg and $\gamma_{t0} = 0$ deg, respectively. The horizontal separation between the missile and the target is 5 km. The defender is launched from the target at the engagement's initiation. To simulate the separation effect, the defender is initiated at a vertical separation of $\Delta y = -10$ m below the target and at a flight-path angle of $\gamma_{d0} \in [-10, 10]$ deg. The target, missile, and defender speeds are $V_t = 300$ m/s, $V_m = 600$ m/s, and $V_d = 600$ m/s, respectively, and their first-order time constants are $\tau_t = 0.5$ s, $\tau_m = 0.2$ s, and $\tau_d = 0.2$ s, respectively. The target's maneuver capability is $a_t^{\max} = 10\ g$ and it performs a bang–bang maximal acceleration maneuver with a single direction switch during the engagement. The missile's maneuver capability is $a_m^{\max} = 25\ g$. The defender's maneuver capability in the sample run is $a_d^{\max} = 25\ g$ and belongs to the closed set $a_d^{\max} \in \{3, 5, 10, 15, 20, 25\}\ g$ in the MC study. The missile is guided to the target using perfect information and one of the following guidance laws: PN, APN, or OGL. The unknown guidance law parameters are the navigation gain for the PN and APN guidance laws and α for the OGL. The guidance law parameters belong to the closed sets $N_i' \in [3, 5]$ for $i = \{\mathrm{PN}, \mathrm{APN}\}$ and $\alpha \in [0, 0.1]$ for OGL.

The initial conditions of the filter are sampled from a Gaussian distribution:

$$\hat{\boldsymbol{x}}_0 \sim \mathcal{N}(\bar{\boldsymbol{x}}_0, \mathbf{P}_0) \tag{65}$$

where $\bar{\boldsymbol{x}}_0$ is the true relative defender–missile initial state and

$$\mathbf{P}_0 = \mathrm{diag}\{50^2, (3\pi/180)^2, (3\pi/180)^2, 10^2, 50^2\} \tag{66}$$

is the initial covariance matrix of the filter.

The MMAC regimes correspond to three possible missile guidance laws belonging to the set {PN, APN, OGL}. The a priori probability of each guidance law is $1/3$. The navigation gains of PN and APN guidance laws are represented by five regimes each, with equal a priori probability:

$$N_i' \in \{3, 3.5, 4, 4.5, 5\}; \qquad i = \mathrm{PN}, \mathrm{APN}$$

For OGL, two regimes with equal probability are considered:

$$\alpha \in \{0, 0.1\}$$

The simulated measurement noise is $\sigma_{\rho i} = 10$ m and $\sigma_{\lambda i} = 1$ m rad, where $i \in \{tm, dm\}$, and the measurement sampling rate is $f_s = 50$ Hz. We assume a blind range of 50 m.

The estimation problem formulation in Sec. II.C and its solution in Sec. III.B address many possible sensor combinations. However, in this simulation study we concentrate on a case in which the defender has bearing-only measurements and the target has both bearing and range measurements, which means that if the defender and target share information, the available measurements are λ_{tm}, ρ_{tm}, and λ_{dm}. This case was chosen due to a number of considerations:

1) The defender is disposable and the system on the aircraft is not; therefore, it is reasonable to invest more in the aircraft sensors than in the defender sensors.

2) The decision to launch a defender by the target would probably require both range and angle from the target.

3) We would like the defender to be as small as possible, which will limit the number of sensors it can carry.

The EOM of the target, missile, and defender are solved using a fourth-order Runge–Kutta algorithm, and the simulation is terminated when the defender passes the missile.

B. Sample Run

This subsection presents a sample run of an APN-guided missile with $N' = 4$ intercepted by a defender missile guided by the OSCOGL presented in Sec. IV. The optimal-switch time t_{sw} is calculated via Eq. (64) at a frequency of 2 Hz. The initial flight-path angles of the missile and defender are $\gamma_{m0} = 20$ deg and $\gamma_{d0} = -10$ deg, respectively.

Figure 5 presents the planar trajectories of the target, missile, and defender in a simulated sample run. The defender's miss distance in this sample run is approximately 0.05 m. Note that the defender's trajectory has very low curvature and does not include an acceleration reversal as with the missile's trajectory. This is due to the fact that the defender is aware beforehand of the planned target maneuver and can anticipate its influence on the trajectory of the incoming homing missile and because the target's switch time was chosen to minimize the defender's control effort. It is also evident that the target maneuvers to lure the missile closer to the defender's trajectory.

Figure 6 presents the posterior probabilities of each guidance law being true and the probability of each guidance law parameter being true as a function of time. Note that after approximately 1 s the APN guidance law has been identified as the missile's guidance law, and after approximately 2 s its navigation gain has also been identified.

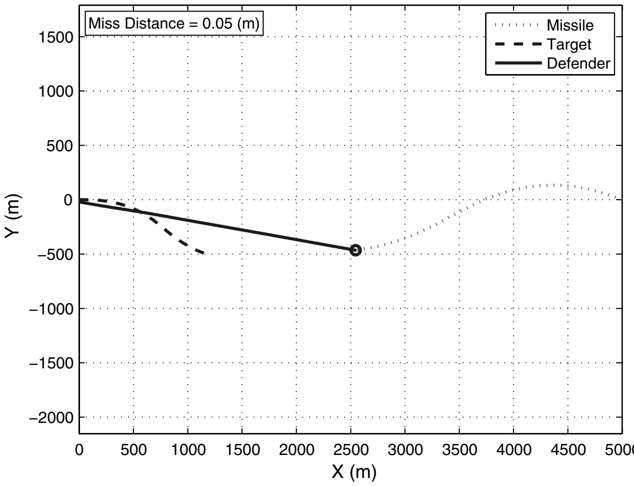

Fig. 5 Sample trajectories. Defender–target team uses OSCOGL. Missile uses APN with $N' = 4$.

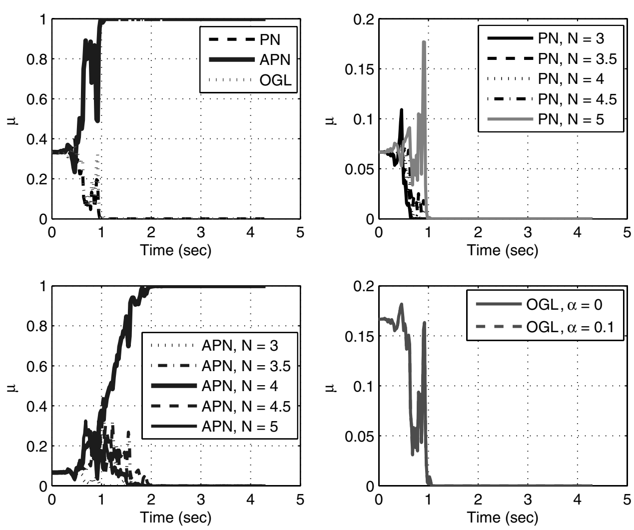

Fig. 6 Sample regime probabilities. Defender–target team uses OSCOGL. Missile uses APN with $N' = 4$.

The identification of the missile's guidance law and navigation gain yields very small estimation errors of the MMAE as can be seen in Fig. 7. Note the fast convergence of all of the estimated states and especially the small error in estimating the missile's acceleration, which is known to have a large effect on miss distance and to be very hard to estimate.

Figure 8 presents the acceleration profiles of the aircraft target, missile, and defender. To intercept the target, performing the 10 g bang–bang maneuver, the missile applies control commands up to approximately 25 g. However, because the target switch time was chosen to minimize the defender's control effort and because after about 2 s the missile's guidance strategy is identified by the target–defender team (see Fig. 6), its entire maneuvering profile until the end of the interception is known. Consequently, the defender does not need to apply more than 4 g in order to intercept it.

C. Monte Carlo Study

A 1000-run Monte Carlo simulation study is used to compare the closed-loop interception performance of the defender missile with and without cooperation in guidance between the target and the defender. In the cooperative mode the COGL (without optimal target switch) and the OSCOGL proposed in Sec. IV are used, whereas in the noncooperative mode an OGL is used. The three guidance laws use the same cooperative estimator. The target performs a bang–bang

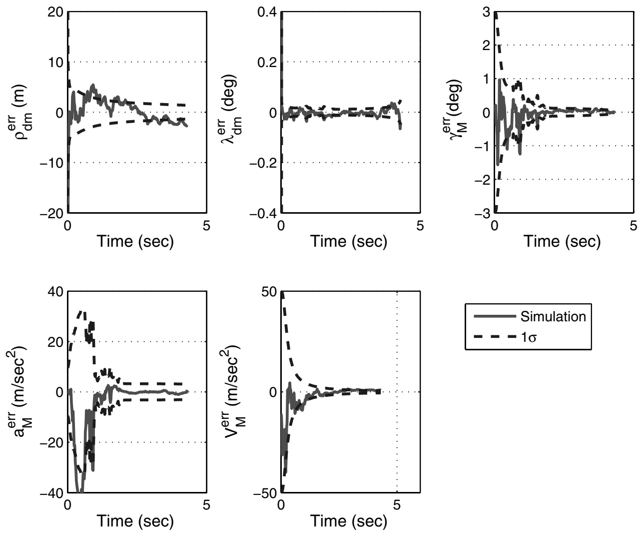

Fig. 7 Sample estimation errors. Defender–target team uses OSCOGL. Missile uses APN with $N' = 4$.

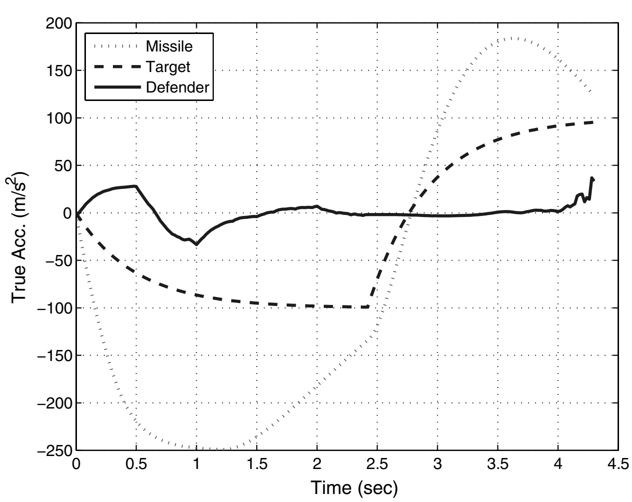

Fig. 8 Sample acceleration profiles. Defender–target team uses OSCOGL. Missile uses APN with $N' = 4$.

maneuver at its maximal acceleration ($a_t = 10\ g$). For COGL and OGL the switch time is chosen to be uniformly distributed over the engagement duration, whereas for the OSCOGL the target switch time is calculated via Eq. (64) at a frequency of 2 Hz. Each run uses random initial conditions and measurement noises sampled from those presented in Sec. V.A and the missile's guidance parameters are chosen from uniform distributions of $N_i' \in [3, 5]$ for $i = \{\text{PN, APN}\}$ and $\alpha \in [0, 0.1]$ for OGL.

Figure 9 presents the miss distance cumulative distribution function (CDF) of the defender using the noncooperative OGL. It is obvious that the performance when using OGL is very poor. Even with $a_d^{\max} = 25$ g, for which the defender has the same maneuver capability as the missile, the required warhead lethality range to ensure a 95% kill probability is more than 25 m. It is also evident that the performance dramatically deteriorates as the defender's acceleration limit is lowered.

Figure 10 presents the miss distance CDF of the defender using the COGL. The required warhead lethality range to ensure a 95% kill probability is 0.19, 0.22, and 0.26 m for $a_d^{\max}$ of 25, 20, and 15 g, respectively. Note that this constitutes hit-to-kill performance and that the performance is still excellent even when the defender's maximal acceleration is 15 g,and the missile's maximal acceleration is 25 g. This is mainly due to the fact the COGL uses the future missile's acceleration profile to optimize the defender's control

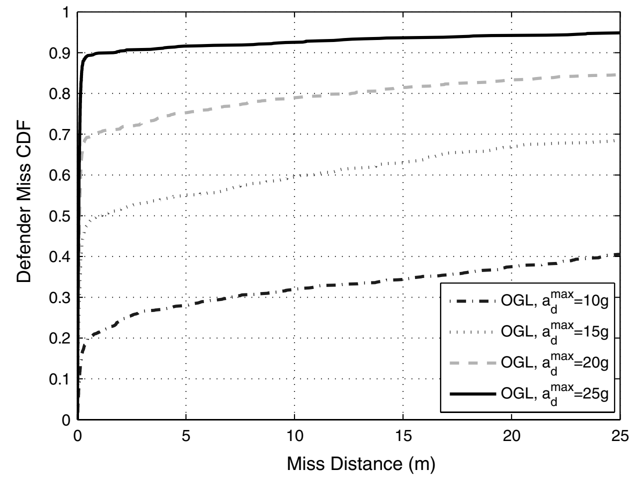

Fig. 9 Monte Carlo analysis. Defender uses OGL.

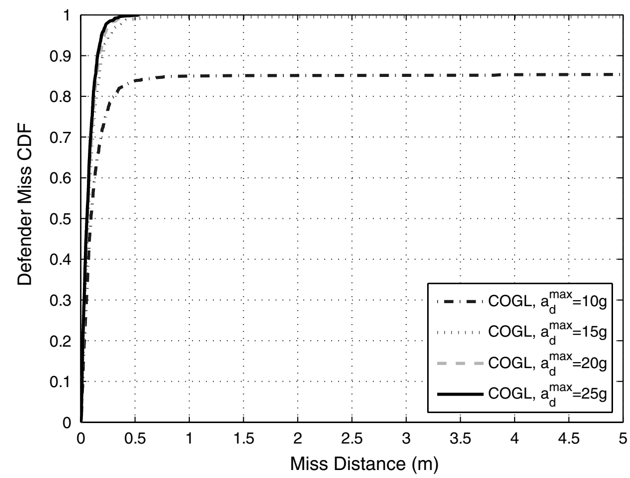

Fig. 10 Monte Carlo analysis. Defender uses COGL.

effort. Although the performance is much better than when using OGL, it is still lacking for an $a_d^{\max}$ of 10 g and lower.

Figure 11 presents the miss distance CDF of the defender using the COGL with an optimal target switch time (the target–defender team uses OSCOGL). The required warhead lethality range to ensure a 95% kill probability is 0.26, 0.36, 0.64, and 1.65 m for $a_d^{\max}$ of 15, 10, 5, and 3 g, respectively. Note that this constitutes hit-to-kill

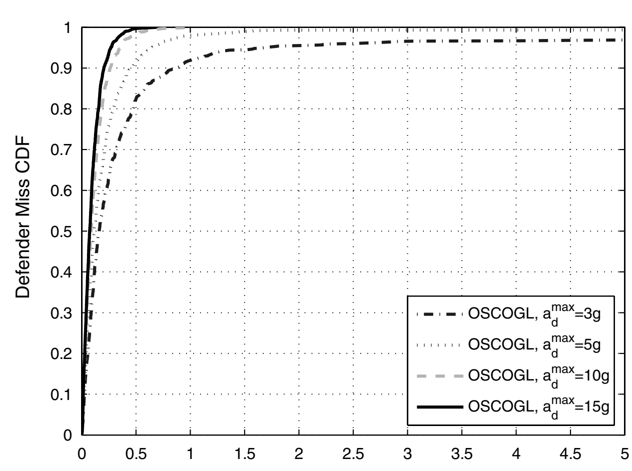

Fig. 11 Monte Carlo analysis. Defender uses COGL. Target performs optimal switch.

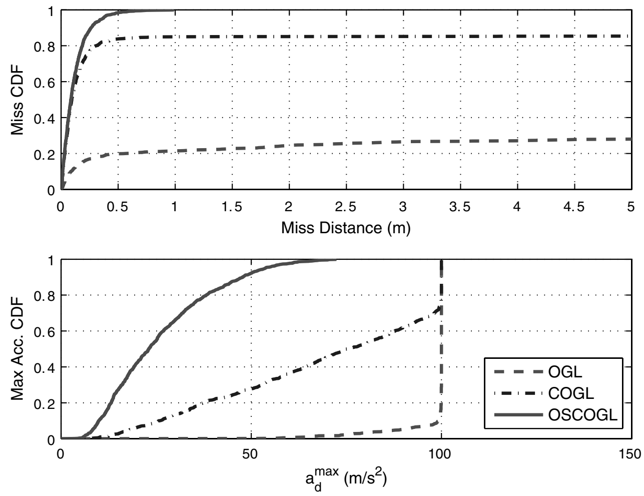

Fig. 12 Monte Carlo analysis. Miss distance and maximal defender acceleration. $a_d^{\max} = 10\ g$.

performance and that the performance is still excellent even when the defender's maximal acceleration is an order of magnitude smaller than that of the missile ($25/3\ g$). This hit-to-kill capability with extremely low control requirements is a result of the optimal target maneuver and the cooperation in guidance between the target and the defender. The extremely small miss distance and the low control requirements can facilitate a small warhead and small rocket engine, lowering the cost and storage space of such a defender missile.

Figure 12 compares the miss distance and maximal acceleration CDFs of the defender when using OGL, COGL, and OSCOGL for $a_d^{\max} = 10\ g$. The plots clarify the reason for the large advantage of the OSCOGL over COGL and OGL. Unlike the OGL and COGL in which the defender saturates with a probability of 0.9 and 0.3, respectively, the OSCOGL does not cause saturation for the same maximal defender accelerations, resulting in the defender's ability to intercept the missile. The OSCOGL does not cause saturation due to the fact that the target switch time is chosen to minimize the defender's control effort and because the defender is aware beforehand to the planned target maneuver and can anticipate its influence on the trajectory of the incoming homing missile.

VI. Conclusions

A cooperative guidance and estimation scheme has been proposed for an interception engagement where a missile is fired from an aircraft to defend it from an incoming homing missile. The proposed multiple-model adaptive control scheme uses for estimation different models to represent the possible homing-missile guidance laws, chosen from a closed set. Fusion of measurements from both the defender missile and protected aircraft was performed. A matched defender's missile guidance law is optimized to the identified homing-missile guidance law. Cooperation in guidance stems from the fact that the defender knows the future evasive maneuvers to be performed by the protected target and the maneuvers it is expected to induce on the incoming homing missile. Moreover, the aircraft can choose a maneuver strategy that helps the defender missile. Extensive Monte Carlo simulations showed the benefit of cooperation.

Regarding guidance, knowing the evasive maneuver of the aircraft substantially reduces the control effort requirements from the defending missile. Choosing an appropriate target maneuver further reduces the defending missile control effort. The cooperation also dramatically improves the defender's homing performance, especially in scenarios in which the target aircraft employs evading maneuvers. For example, in a representative sample scenario, the target aircraft performs a $10\ g$ bang–bang evasive maneuver, inducing up to $25\ g$ maneuvers from the homing missile. In comparison, the defender–missile maneuvers did not exceed $4\ g$, while still enabling near-zero miss distance.

From the estimation perspective, fusion of measurements between the aircraft and defending missile enables fast identification of the missile's guidance strategy, making its future trajectory predictable. Moreover, in cases in which the defending missile has bearing-only measurements, the cooperation with the aircraft also enables estimating range, and thus advanced cooperative optimal-control-based guidance laws can be used.

Such cooperation in guidance and estimation enables hit-to-kill performance from a defending missile having a very limited maneuver capability and carrying sensors that provide bearing-only measurements. This facilitates the use of relatively small defending missiles to protect aircraft from homing missiles.

Acknowledgments

This effort was sponsored by the U.S. Air Force Office of Scientific Research, Air Force Material Command, under grant number FA8655-09-1-3051. The U.S. Government is authorized to reproduce and distribute reprints for Governmental purpose notwithstanding any copyright notation thereon.

Appendix: Dynamics Jacobian Partial Derivatives

This Appendix presents the partial derivatives of u_m with respect to the states for the PN, APN, and OGL. These are employed in the Jacobian matrix of Eq. (32).

I. Proportional Navigation

The partial derivatives of u_m for the PN guidance law are

$$\frac{\partial u_m^{\mathrm{PN}}}{\partial \rho_{dm}} = \frac{N'(\Delta_1\Delta_2 - V_{\lambda tm}V_{\rho tm}\Delta_3)}{\rho_{tm}^3\cos(\gamma_m + \lambda_{tm})} \tag{A1}$$

$$\frac{\partial u_m^{\mathrm{PN}}}{\partial \lambda_{dm}} = \frac{N'\rho_{dm}(\Delta_1\Delta_3 + V_{\lambda tm}V_{\rho tm}\Delta_2)}{\rho_{tm}^3\cos(\gamma_m + \lambda_{tm})} \tag{A2}$$

$$\frac{\partial u_m^{\mathrm{PN}}}{\partial \gamma_m} = \frac{N'}{\rho_{tm}}\left[V_m V_{\lambda tm}\tan(\gamma_m + \lambda_{tm}) + V_{\rho tm}V_m + V_{\rho tm}V_{\lambda tm}\frac{\tan(\gamma_m + \lambda_{tm})}{\cos(\gamma_m + \lambda_{tm})}\right] \tag{A3}$$

$$\frac{\partial u_m^{\mathrm{PN}}}{\partial a_m} = 0 \tag{A4}$$

$$\frac{\partial u_m^{\mathrm{PN}}}{\partial V_m} = \frac{N'[V_{\rho tm}\tan(\gamma_m + \lambda_{tm}) - V_{\lambda tm}]}{\rho_{tm}} \tag{A5}$$

where

$$\Delta_1 = (V_{\lambda tm}^2 + V_{\lambda tm}V_{\rho tm}\tan(\gamma_m + \lambda_{tm}) - V_{\rho tm}^2) \tag{A6}$$

$$\Delta_2 = [\Delta X_{tm}\sin(\lambda_{dm}) - \Delta Y_{tm}\cos(\lambda_{dm})] \tag{A7}$$

$$\Delta_3 = [\Delta X_{tm}\cos(\lambda_{dm}) + \Delta Y_{tm}\sin(\lambda_{dm})] \tag{A8}$$

$V_{\rho tm}$ and $V_{\lambda tm}$ are calculated via Eqs. (4), ΔX_{tm} and ΔY_{tm} are defined in Eqs. (17), and ρ_{tm} and λ_{tm} are given by Eq. (29).

II. Augmented Proportional Navigation

The partial derivatives of u_m for the APN guidance law are

$$\frac{\partial u_m^{\mathrm{APN}}}{\partial \rho_{dm}} = \frac{\partial u_m^{\mathrm{PN}}}{\partial \rho_{dm}} + \frac{N' \Delta_2 a_t \sin(\gamma_t + \gamma_m)}{2\rho_{tm}^2 \cos^2(\gamma_m + \lambda_{tm})} \tag{A9}$$

$$\frac{\partial u_m^{\mathrm{APN}}}{\partial \lambda_{dm}} = \frac{\partial u_m^{\mathrm{PN}}}{\partial \lambda_{dm}} + \frac{N' \Delta_3 a_t \rho_{dm} \sin(\gamma_t + \gamma_m)}{2\rho_{tm}^2 \cos^2(\gamma_m + \lambda_{tm})} \tag{A10}$$

$$\frac{\partial u_m^{\mathrm{APN}}}{\partial \gamma_m} = \frac{\partial u_m^{\mathrm{PN}}}{\partial \gamma_m} + \frac{N' a_t \cos(\gamma_t - \lambda_{tm}) \tan(\gamma_m + \lambda_{tm})}{2\cos(\gamma_m + \lambda_{tm})} \tag{A11}$$

$$\frac{\partial u_m^{\mathrm{APN}}}{\partial a_m} = 0 \tag{A12}$$

$$\frac{\partial u_m^{\mathrm{APN}}}{\partial V_m} = \frac{\partial u_m^{\mathrm{PN}}}{\partial V_m} \tag{A13}$$

III. Optimal Guidance Law

The partial derivatives of u_m for the OGL are

$$\frac{\partial u_m^{\mathrm{OGL}}}{\partial \rho_{dm}} = \frac{\partial u_m^{\mathrm{APN}}}{\partial \rho_{dm}} + \frac{1}{\tau_m}\left[\frac{u_m^{\mathrm{APN}}}{N'}\left(\frac{\partial N'}{\partial \theta}\right) - a_m\left(\frac{\partial \bar{N}}{\partial \theta}\right)\right]\left(\frac{\partial t_{\mathrm{go}}^{tm}}{\partial \rho_{dm}}\right) \tag{A14}$$

$$\frac{\partial u_m^{\mathrm{OGL}}}{\partial \lambda_{dm}} = \frac{\partial u_m^{\mathrm{APN}}}{\partial \lambda_{dm}} + \frac{1}{\tau_m}\left[\frac{u_m^{\mathrm{APN}}}{N'}\left(\frac{\partial N'}{\partial \theta}\right) - a_m\left(\frac{\partial \bar{N}}{\partial \theta}\right)\right]\left(\frac{\partial t_{\mathrm{go}}^{tm}}{\partial \lambda_{dm}}\right) \tag{A15}$$

$$\frac{\partial u_m^{\mathrm{OGL}}}{\partial \gamma_m} = \frac{\partial u_m^{\mathrm{APN}}}{\partial \gamma_m} + \frac{1}{\tau_m}\left[\frac{u_m^{\mathrm{APN}}}{N'}\left(\frac{\partial N'}{\partial \theta}\right) - a_m\left(\frac{\partial \bar{N}}{\partial \theta}\right)\right]\left(\frac{\partial t_{\mathrm{go}}^{tm}}{\partial \gamma_m}\right) \tag{A16}$$

$$\frac{\partial u_m^{\mathrm{OGL}}}{\partial a_m} = -\bar{N} \tag{A17}$$

$$\frac{\partial u_m^{\mathrm{OGL}}}{\partial V_m} = \frac{\partial u_m^{\mathrm{APN}}}{\partial V_m} + \frac{1}{\tau_m}\left[\frac{u_m^{\mathrm{APN}}}{N'}\left(\frac{\partial N'}{\partial \theta}\right) - a_m\left(\frac{\partial \bar{N}}{\partial \theta}\right)\right]\left(\frac{\partial t_{\mathrm{go}}^{tm}}{\partial V_m}\right) \tag{A18}$$

where

$$\frac{\partial N'}{\partial \theta} = \frac{A(\theta) - B(\theta)}{D^2(\theta)} \tag{A19}$$

$$A(\theta) = 6(2\theta \exp(-\theta) - \theta^2 \exp(-\theta) + 3\theta^2 - 2\theta)D(\theta) \tag{A20}$$

$$B(\theta) = 36\theta^2 \psi(\theta)(1 - 2\theta + \theta^2 - 2\exp(-\theta) + 2\theta \exp(-\theta) + \exp(-2\theta)) \tag{A21}$$

$$D(\theta) = 3 + 6\theta - 6\theta^2 + 2\theta^3 - 3\exp(-2\theta) - 12\theta \exp(-\theta) + 6\alpha/\tau_m^3 \tag{A22}$$

$$\frac{\partial \bar{N}}{\partial \theta} = \frac{12\psi(\theta)(1 - \exp(-\theta))D(\theta) - 6\psi^2(\theta)[\frac{\partial D(\theta)}{\partial \theta}]}{D^2(\theta)}, \qquad \bar{N} = \frac{6\psi^2(\theta)}{D(\theta)} \tag{A23}$$

$$\frac{\partial D(\theta)}{\partial \theta} = 6(1 - 2\theta + \theta^2 + \exp(-2\theta) - 2\exp(-\theta) + 2\theta \exp(-\theta)) \tag{A24}$$

and

$$\frac{\partial t_{\mathrm{go}}^{tm}}{\partial \rho_{dm}} = \frac{V_{\lambda tm}\Delta_2 - V_{\rho tm}\Delta_3}{\rho_{tm} V_{\rho tm}^2} \tag{A25}$$

$$\frac{\partial t_{\mathrm{go}}^{tm}}{\partial \lambda_{dm}} = \frac{\rho_{dm}(V_{\lambda tm}\Delta_3 + V_{\rho tm}\Delta_2)}{\rho_{tm} V_{\rho tm}^2} \tag{A26}$$

$$\frac{\partial t_{\mathrm{go}}^{tm}}{\partial \gamma_m} = \frac{\rho_{tm} V_m \sin(\gamma_m + \lambda_{tm})}{V_{\rho tm}^2} \tag{A27}$$

$$\frac{\partial t_{\mathrm{go}}^{tm}}{\partial V_m} = -\frac{\rho_{tm} \cos(\gamma_m + \lambda_{tm})}{V_{\rho tm}^2} \tag{A28}$$

References

[1] Zarchan, P., *Tactical and Strategic Missile Guidance*, Vol. 157, Progress in Astronautics and Aeronautics, AIAA, Washington D.C., 1994.

[2] Garber, V., "Optimum Intercept Laws for Accelerating Targets," *AIAA Journal*, Vol. 6, No. 11, 1968, pp. 2196–2198. doi:10.2514/3.4962

[3] Cottrell, G. R., "Optimal Intercept Guidance for Short-Range Tactical Missiles," *AIAA Journal*, Vol. 9, No. 7, 1971, pp. 1414–1415. doi:10.2514/3.6369

[4] Bryson, E. A., and Ho, C. Y., *Applied Optimal Control*, Blaisdell, Waltham, MA, 1969.

[5] Ben-Asher, J. Z., and Yaesh, I., *Advances in Missile Guidance Theory*, Vol. 180, Progress in Astronautics and Aeronautics, AIAA, Reston, VA, 1998, pp. 25–32.

[6] Gutman, S., "On Optimal Guidance for Homing Missiles," *Journal of Guidance and Control*, Vol. 2, No. 4, 1979, pp. 296–300. doi:10.2514/3.55878

[7] Shinar, J., "Solution Techniques for Realistic Pursuit-Evasion Games," *Advances in Control and Dynamic Systems*, edited by C. T. Leondes, Vol. 17, Academic Press, New York, 1981, pp. 63–124.

[8] Isaacs, R., *Differential Games*, Wiley, New York, 1965.

[9] Ho, C. Y., and Bryson, E. A., "Differential Games and Optimal Pursuit-Evasion Strategies," *IEEE Transactions on Automatic Control*, Vol. AC-10, No. 4, 1965, pp. 385–389. doi:10.1109/TAC.1965.1098197

[10] Julich, P. M., and Borg, D. A., "Proportional Navigation vs an Optimally Evading Constant-Speed Target in Two Dimension," *Journal of Spacecraft and Rockets*, Vol. 7, No. 12, 1970, pp. 1454–1457. doi:10.2514/3.30190

[11] Slater, G. L., and Wells, W. R., "Optimal Evasive Tactics Against a Proportional Navigation Missile with Time Delay," *Journal of Spacecraft and Rockets*, Vol. 10, No. 5, 1973, pp. 309–313. doi:10.2514/3.27759

[12] Shinar, J., and Steinberg, D., "Analysis of Optimal Evasive Maneuvers Based on a Linearized Two-Dimensional Kinematic Model," *Journal of Aircraft*, Vol. 14, No. 8, 1977, pp. 795–802. doi:10.2514/3.58855

[13] Shinar, J., Rotsztein, Y., and Bezner, E., "Analysis of Three-Dimensional Optimal Evasion with Linearized Kinematics," *Journal of Guidance and Control*, Vol. 2, No. 5, 1979, pp. 353–360. doi:10.2514/3.55889

[14] Shinar, J., and Gutman, S., "The Effects of Non-Linear Kinematics in Optimal Evasion," *Optimal Control Applications and Methods*, Vol. 4, No. 2, 1983, pp. 139–152. doi:10.1002/oca.4660040204

[15] Imado, F., and Miwa, S., "Fighter Evasive Maneuvres Against Proportional Navigation Missile," *Journal of Aircraft*, Vol. 23, No. 11, 1986, pp. 825–830. doi:10.2514/3.45388

[16] Ben-Asher, Z. J., and Cliff, M. E., "Optimal Evasion Against a Proportionally Guided Pursuer," *Journal of Guidance, Control, and Dynamics*, Vol. 12, No. 4, 1989, pp. 598–600.
doi:10.2514/3.20450
[17] Shinar, J., and Tabak, R., "New Results in Optimal Missile Avoidance Analysis," *Journal of Guidance, Control, and Dynamics*, Vol. 17, No. 5, 1994, pp. 897–902.
doi:10.2514/3.21287
[18] Speyer, J. L., "An Adaptive Terminal Guidance Scheme Based on Exponential Cost Criterion with Application to Homing Missile Guidance," *IEEE Transactions on Automatic Control*, Vol. AC-21, No. 3, 1976, pp. 371–375.
doi:10.1109/TAC.1976.1101206
[19] Fitzgerald, R. J., and Zarchan, P., "Shaping Filters for Randomly Initiated Target Maneuvers," *Proceedings of the AIAA Guidance and Control Conference*, AIAA, New York, 1978, pp. 424–430.
[20] Bezner, E., and Shinar, J., "Optimal Evasive Maneuvers in Conditions of Uncertainty," *Proceedings of the 22nd Israel Annual Conference on Aviation and Astronautics*, 1980, pp. 185–186.
[21] Zarchan, P., "Proportional Navigation and Weaving Targets," *Journal of Guidance, Control, and Dynamics*, Vol. 18, No. 5, 1995, pp. 969–974.
doi:10.2514/3.21492
[22] Ohlmeyer, J. E., "Root-Mean-Square Miss Distance of Proportional Navigation Missile Against Sinusoidal Target," *Journal of Guidance, Control, and Dynamics*, Vol. 19, No. 3, 1996, pp. 563–568.
doi:10.2514/3.21658
[23] Shinar, J., and Gutman, S., "Three-Dimensional Optimal Pursuit and Evasion with Bounded Controls," *IEEE Transactions on Automatic Control*, Vol. 25, No. 3, 1980, pp. 492–496.
doi:10.1109/TAC.1980.1102372
[24] Lin, L., Kirubarjan, T., and Bar-Shalom, Y., "Pursuer Identification and Time-to-Go Estimation Using Passive Measurments from an Evader," *IEEE Transactions on Aerospace and Electronic Systems*, Vol. 41, No. 1, 2005, pp. 190–204.
doi:10.1109/TAES.2005.1413756
[25] Karelahti, J., and Virtanen, K., "Adaptive Controller for the Avoidance of an Unknownly Guided Air Combat Missile," *Proceedings of the 46th IEEE Conference on Decision and Control*, Inst. of Electrical and Electronics Engineers, Piscataway, NJ, 2007, pp. 1306–1313.
[26] Asher, R., and Matuszewski, J., "Optimal Guidance with Maneuvering Targets," *Journal of Spacecraft and Rockets*, Vol. 11, No. 3, 1974, pp. 204–206.
doi:10.2514/3.62041
[27] Boyell, L. R., "Defending a Moving Target Against Missile or Torpedo Attack," *IEEE Transactions on Aerospace and Electronic Systems*, Vol. AES-12, No. 4, 1976, pp. 522–526.
doi:10.1109/TAES.1976.308338
[28] Shinar, J., and Silberman, G., "A Discrete Dynamic Game Modeling Anti-Missile Defence Scenarios," *Dynamics and Control*, Vol. 5, No. 1, 1995, pp. 55–67.
doi:10.1007/BF01968535
[29] Lipman, Y., and Shinar, J., "Mixed-Strategy Guidance in Future Ship Defense," *Journal of Guidance, Control, and Dynamics*, Vol. 19, No. 2, 1996, pp. 334–339.
doi:10.2514/3.21623
[30] Rusnak, I., "Guidance Laws in Defense Against Missile Attack," *Proceedings of the IEEE 25th Convention of Electrical and Electronic Engineers in Israel*, Inst. of Electrical and Electronics Engineers, Piscataway, NJ, 2008, pp. 90–94.
[31] Magill, T. D., "Optimal Adaptive Estimation of Sampled Stochastic Processes," *IEEE Transactions on Automatic Control*, Vol. 10, No. 4, 1965, pp. 434–439.
doi:10.1109/TAC.1965.1098191
[32] Sims, F. L., and Lainiotis, D. G., "Recursive Algorithm for the Calculation of the Adaptive Kalman Filter Weighting Coeffcients," *IEEE Transactions on Automatic Control*, Vol. 14, No. 2, 1969, pp. 215–218.
doi:10.1109/TAC.1969.1099155
[33] Oshman, Y., Shinar, J., and Avrashi, W. S., "Using a Multiple Model Adaptive Estimator in Random Evasion Missile/Aircraft Encounter," *Journal of Guidance, Control, and Dynamics*, Vol. 24, No. 6, 2001, pp. 1176–1186.
doi:10.2514/2.4833
[34] Shima, T., Oshman, Y., and Shinar, J., "Efficient Multiple Model Adaptive Estimation in Ballistic Missile Interception Scenarios," *Journal of Guidance, Control, and Dynamics*, Vol. 25, No. 4, 2002, pp. 667–675.
doi:10.2514/2.4961
[35] Lainiotis, D. G., "Partitioning: A Unifying Framework for Adaptive Systems, II: Control," *Proceedings of the IEEE*, Vol. 64, No. 8, 1976, pp. 1182–1198.
doi:10.1109/PROC.1976.10289
[36] Rusnak, I., "Multiple Model-Based Terminal Guidance Law," *Journal of Guidance, Control, and Dynamics*, Vol. 23, No. 4, 2000, pp. 742–746.
doi:10.2514/2.4593
[37] Bar-Shalom, Y., Rong Li, X., and Kirubarajan, T., *Estimation with Applications to Tracking and Navigation*, Wiley, New York, 2001, pp. 453–460.
[38] Gutman, S., *Applied Min-Max Approach to Missile Guidance and Control*, Vol. 2009, AIAA, New York, 2005.